MEASUREMENT AND PROCESSING OF INDOOR GPS SIGNALS USING A ONE-SHOT SOFTWARE RECEIVER

Gustavo López-Risueño, Gonzalo Seco-Granados
TT&C and Navigation Section (TEC-ETT), Electrical Engineering Department
ESTEC, European Space Agency
Keplerlaan 1, 2201 AZ Noordwijk ZH, The Netherlands
***Phone* +31 715658562, *Fax* +31 715654596**
email:{gustavo.lopez.risueno,gonzalo.seco.granados}@esa.int

Abstract

A One-Shot receiver for indoor positioning using the GPS L1 C/A signal is presented. It uses both coherent correlation and noncoherent integration to achieve the low sensitivity required for indoor applications, and includes interpolation for code delay estimation, a novel CN_0 estimator, and a near-far problem mitigation technique. The impact of the navigation message bit transitions on the sensitivity is also studied. Live indoor environments are used to show the receiver performance.

1 INTRODUCTION

The US FCC's mandate E911 and the European recommendation E112, both regulating and specifying the positioning of emergency callers, have represented the starting point for the extensive deployment of location-based services LBS in cellular networks. LBS are viewed as an important source of revenues for cellular network operators in the near future, and constitute an excellent opportunity for the Global Navigation Satellite System (GNSS) industry to enter a massive market that can boost the demand of GNSS receivers and applications [1, 2]. To meet the requirements of LBS (roughly speaking, positioning errors equal or less than 100 m and time to fix below 30 sec), strictly cellular-based technologies have been considered, such as the Cell Identification (Cell-ID) and the Enhanced Observed Time Difference (E-OTD) [3, 4]. On the one hand, Cell-ID does not hold the required positioning accuracy unless the caller is in a micro- or pico- cell. On the other hand, E-OTD can achieve the required accuracy but needs 3 or more base stations, this being a major drawback in rural areas. GNSS can provide the required accuracy in most locations, including those where the above-mentioned techniques fail. Beside its wide coverage, the use of GNSS encompasses other important advantages: much better accuracy than specified in many environments (on the order of tens of metres), matureness of the technology, low operators' deployment cost, and user privacy [1, 2, 5, 6]. For those reasons, GNSS is considered to be a very adequate enabler of LBS in cellular networks. Further, the current GNSS performance will be improved by the deployment of Galileo.

Nevertheless, conventional GNSS receivers perform poorly in dense urban environments (urban canyons) and indoor sites [5, 6], since they rely on processing line of sight (LOS) satellite signals with low attenuation (with respect to the specified signal level), and low or moderate multipath. The signal propagation in urban canyons and indoors can be, however, subject to high attenuation, very different attenuation patterns, severe multipath, and even non-LOS conditions [7, 8]. Particularly, the fact that signals coming from different satellites suffer from very different attenuation patterns causes the appearance of the near-far problem, typical of code division multiple-access communications [9]. This problem does not arise in conventional GNSS environments since, unless pseudolites are used [10], all satellite signals approximately hold the same power at the receiver antenna. An additional drawback of conventional GNSS techniques is the time to first fix (a few minutes), which is much greater then the required one in LBS [2].

To overcome the last problem, assistance data can be sent to the user through the mobile network. By this technology, so-called Assisted GNSS (A-GNSS) [11, 12], the user GNSS receiver is provided with information on

the visible satellites, their approximate Doppler frequency and code delay, ephemeris, the navigation message, etc, that are measured by a reference receiver in the vicinity of the user. A-GNSS reduces the time to fix to less than 20 sec, requires a lower computational burden than standalone GNSS, and improves the acquisition sensitivity. The high attenuation of the signals in urban canyons and indoor sites can be mitigated by the use of a receiver architecture known as High Sensitivity GNSS receiver (HS-GNSS), extensively investigated for GPS [5, 7, 8]. HS-GNSS main feature is the use of both coherent and non-coherent code correlation over long periods of several seconds in order to improve the sensitivity. The required sensitivity is around 15 dBHz carrier-to-noise ratio (CN_0) for indoor and 20 dBHz for urban canyons [11, 12]. HS-GNSS receivers are intimately related to the use of A-GNSS, since 1) non-coherent integration implies the destruction of the navigation message on the signal; and 2) A-GNSS alleviates the great computational burden of this type of receivers by reducing the search in code delay and Doppler. For static applications, A-GNSS can even help extend the coherent correlation time above the bit period [11, 12]. The near-far and the multipath problems in urban canyons and indoor sites have, however, remained quite unexplored in the GNSS literature (a few papers can be found: [8] on the near-far problem mitigation, [7] on the multipath).

This paper describes a One-Shot receiver based on the HS-GNSS principle and shows its performance both in simulated and live indoor environments. A One-shot receiver works on single blocks of sampled GNSS signals and only incorporates the acquisition stage of a standard receiver, being very adequate for the integration in mobile units. The paper analyses important aspects of the HS-GNSS principle, such as the sampling rate, the interpolation for code delay estimation, and the impact of the navigation message bit transitions on the sensitivity. It also presents a novel CN_0 estimator suitable for low-CN_0 environments that can be used in the weighted least squares solution of the position [11, 12], and a near-far mitigation algorithm comprising a novel near-far problem detector and a multiuser detection technique [9, 10]; the CN_0 estimator is also needed in the near-far problem mitigation algorithm. The paper deals with indoor environments, since they suffer from the same problems as urban canyons but to a greater extent, and focus on the GPS L1 C/A signal; the extension of the results obtained to the Galileo signal structure is addressed at the end of the paper. The rest of the paper is organized as follows. Section 2 describes the signal model. Section 3 deals with the principles of the HS-GNSS receivers. Section 4 is devoted to the CN_0 estimation. The near-far problem mitigation algorithm is presented in Section 5. The experimental results for indoor positioning are shown in Section 6. Finally, the conclusions are drawn in Section 7.

2 SIGNAL MODEL

The GPS L1 C/A signal transmitted by the ith satellite can be modeled as

$$s_i(t) = \sum_{r_1=-\infty}^{\infty} b_i(r_1) \sum_{r_2=0}^{N_b L_c - 1} a_i\left((r_2)_{L_c}\right)\ p_{T_c}\left(t - r_2\ T_c - r_1\ T_b\right) \tag{1}$$

where zero Doppler, no noise and no multipath have been assumed. The sequence $\{b_i(r) = \pm 1\}$ constitutes the navigation message, $\{a_i(r)\}_{r=0}^{L_c-1}$ is the corresponding L_c-sample spreading code, and $(x)_L$ means the modulo-L of x. T_b and T_c are respectively the bit and chip duration, and N_b is the number of code epochs per bit; in this case: $T_b = L_c T_c N_b$; $L_c = 1023$, $T_c = 1/f_c$ and $f_c = 1.023$ MHz, and $N_b = 20$. The signal $p_{T_c}(t)$ is a unit-power chip shaping pulse, i.e. $\frac{1}{T_c} \int |p_{T_c}(t)|^2\ dt = 1$. For M satellite signals impinging on the receiver, the complex-envelope model of the input signal follows

$$x(t) = \sum_{i=1}^{M} \left[A_i\ e^{j(2\pi f_i t + \phi_i)} \left(s_i(t - \tau_i) + \sum_{j=1}^{R_i} \alpha_{i,j}\ s_i(t - \theta_{i,j})\ e^{j(2\pi \Delta f_{i,j}\ t + \Delta\phi_{i,j})} \right) \right] + w(t), \tag{2}$$

where $s_i(t-\tau_i)$ is the first arriving signal from the ith satellite with the corresponding code delay τ_i, amplitude A_i and Doppler frequency f_i. Due to the propagation conditions in indoor environments, the amplitude will widely vary from satellite to satellite. We also assume R_i additional reflected rays impinging at the receiver with code delay $\theta_{i,j}$, Doppler offset $\Delta f_{i,j}$ and relative amplitude $\alpha_{i,j}$. The noise term ($w(t)$) is modelled as a zero-mean, circularly-complex white Gaussian process with bilateral spectral density $2N_0$. The CN_0 for the ith satellite is then defined as $\mathrm{CN}_{0i} = A_i^2/2N_0$. The role of the indoor receiver is to find the satellites present, and estimate their code delays ($\{\tau_i\}_{i=1}^M$) and CN_0 ($\{\mathrm{CN}_{0i}\}_{i=1}^M$).

3 HIGH SENSITIVITY GNSS RECEIVERS

As pointed out in the Introduction, HS-GNSS receivers [5, 7, 8] combine coherent correlation and non-coherent integration during long periods in order to improve the sensitivity in the satellite signal acquisition. Non-coherent integration holds less processing gain than coherent correlation; however, it overcomes the limitations of the coherent correlation over long periods, i.e. bit transitions in the navigation message, user dynamics, and user clock misbehavior [8, 13]. The acquisition phase of a HS-GNSS is summarized as follows: To acquire the ith satellite, the input signal is demodulated by a Doppler frequency and crosscorrelated with a delayed ith satellite signal code replica. For a particular code delay (τ) and Doppler frequency (f) cell, the HS-GNSS obtains the following squared crosscorrelation:

$$X_i(\tau, f) = \frac{1}{N_I} \sum_{r=0}^{N_i-1} \left| \int_{rL_cT_cN_c}^{(r+1)L_cT_cN_c} x(t)\ c_i(t-\tau)\ e^{-j2\pi f\ t}\ dt \right|^2, \tag{3}$$

where N_c is the number of code epochs coherently correlated, N_I the number of correlation blocks noncoherently integrated, and $c_i(t-\tau)$ is the delayed code replica: $c_i(t) = \sum_{r=0}^{L_cN_c-1} a_i\left((r)_{L_c}\right)\ p_{T_c}\left(t - r\ T_c\right)$. The **coherent correlation time** is $L_cT_cN_c$, and the total **dwell time** is $L_cT_cN_cN_I$. The ith satellite is acquired when the cross-correlation $X_i(\tau, f)$ surpasses a given threshold (Th) for any delay-Doppler cell; the code delay and Doppler frequency estimators take on

$$\left(\widehat{\tau}_i, \widehat{f}_i\right) = \underset{\{(\tau,f):\ X_i(\tau,f)>Th\}}{\arg\max} \{X_i(\tau, f)\}. \tag{4}$$

The threshold Th is set to meet a given probability of false alarm $\mathrm{P_{FA}}$ (when only noise is present). The sensitivity to acquire a satellite signal is defined as the minimum $\mathrm{CN_0}$ to detect it with a probability of detection $\mathrm{P_D}$ given a probability of false alarm $\mathrm{P_{FA}}$. The sensitivity of a HS-GPS receiver is shown in Fig. 1 for several coherent correlation and noncoherent integration lengths ($\mathrm{P_D} = 90\%$, $\mathrm{P_{FA}} = 10^{-6}$). Note that, to achieve an adequate sensitivity for indoor positioning (around $\mathrm{CN_0} = 15$ dBHz), it should be necessary to process several seconds of signal: 5 sec if $N_c = 5$, $N_I = 1000$; 2 sec if $N_c = 20$, $N_I = 100$; or 1.6 sec if $N_c = 40$, $N_I = 40$. Beside, the coherent correlation of more than 20 ms of coherent correlation would require data-aided techniques in order to strip off the bit transitions (possible if A-GNSS is used [11, 12]).

The effects of the bit transitions deserves special attention. Clearly, when using only very long coherent correlation times, bit transitions cause sensitivity losses and may result in false acquisitions. Although HS-GNSS receivers do not typically perform very long coherent correlations, they hold very long dwell times, so that a bit transitions will be likely to appear in several coherent correlation blocks. For instance, a HS-GPS receiver with $N_c = 5$, $N_I = 1000$ presents a dwell time of 5 sec; thus there can be up to 249 bit transitions. We have concluded that, for HS-GNSS receivers, bit transitions mainly result in sensitivity losses as well, the mean and the worst-case losses being

$$\overline{L} = -10\log_{10}\left(1 - \frac{L_cT_cN_c}{3\ T_b}\right), \quad L_{wc} = -10\log_{10}\left(1 - \frac{L_cT_cN_c}{T_b}\right). \tag{5}$$

Note that 1) neither the mean nor the worst-case expressions depend on the number of noncoherently integrated blocks but on the coherent correlation time, 2) L_{wc} becomes infinity when the coherent correlation time approaches T_b. Both expressions are valid for coherent correlation time below T_b and dwell times greater than T_b. For the case of the GPS L1 C/A signal, these losses are depicted in Fig. 2. Both the mean and worst-case losses are small below 5 ms coherent correlation. Although the mean losses remain small even for 20 ms coherent correlation, the worst-case losses turn out very high from 10 ms onwards.

We only have dealt with acquisition due to the focus on One-Shot receivers. For the sake of computational efficiency, One-Shot receivers use interpolation rather than tracking after acquisition. In the sequel, the effects of sampling and the interpolation to refine the code delay estimation of (4) are discussed. The details on the implementation of the HS-GNSS are also treated.

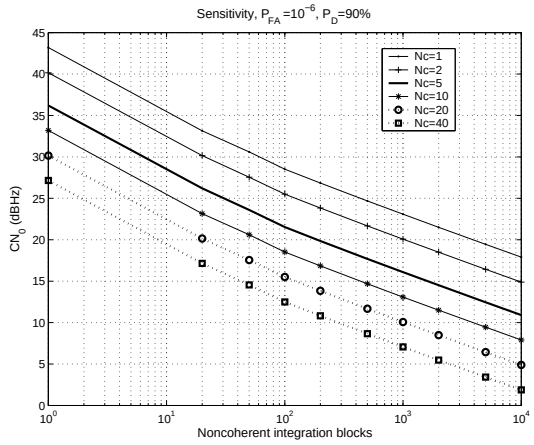

Figure 1: HS-GPS receiver sensitivity (CN_0) for different correlation and noncoherent integration times ($P_{FA} = 10^{-6}$, $P_D = 90\%$).

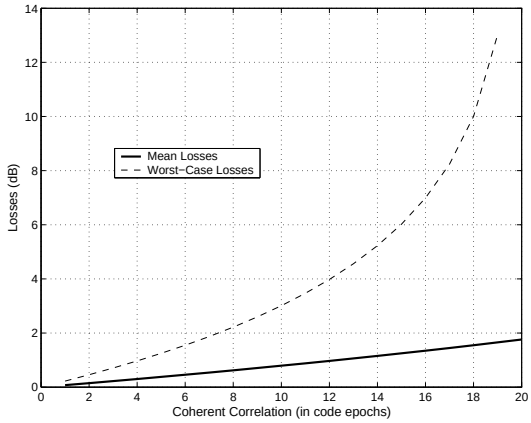

Figure 2: Losses in sensitivity for a HS-GPS receiver due to bit transitions in the navigation message.

3.1 Sampling, interpolation, and implementation details

The digital implementation of HS-GNSS receivers requires the selection of the sampling rate. A sampling rate equal to an integer number of times the bit or chip rate (i.e. a **commensurate sampling rate**) is usually encountered in digital communication receivers. However, this is not adequate for GNSS receivers in general, since the ultimate timing resolution is limited to the sample period, this compromising the final position estimation. Therefore, the use of **non-commensurate sampling** should be considered [14]. In non-commensurate sampling, the sampling frequency (f_s) and the chip rate (f_c) are related by

$$\frac{f_s}{f_c} = \frac{p}{q}, \tag{6}$$

where p and q are two prime positive integers greater than 1. The timing resolution becomes T_c/p, and is achieved when processing more than q chips. In general, it is desirable a high p and a not very high p/q ratio in order to avoid high sampling rates. The effect of the non-commensurate sampling on the computation of the squared crosscorrelation of (3) is illustrated for a GPS L1 C/A signal in Fig. 3. If a non-commensurate sampling is used ($f_s = 5.4558$ MHz), the computed crosscorrelation matches the theoretical one; however, for a commensurate sampling ($fs = 4 \cdot f_c$), the computed crosscorrelation is a staircase-like approximation of the ideal one, the step width being the sampling period (1/4 chips in this example). For the non-commensurate example, the ratio p/q is 9093/1705, so that more than one code epoch must be processed to obtain a resolution of 1/9093 chips. In fact, 5 epochs are used.

Despite the excellent resolution achievable by means of non-commensurate sampling, the ultimate precision in the code delay estimation for the One-Shot receiver would be the sampling period, since the receiver computes a sampled version of the crosscorrelation of Fig. 3. That is, $X_i(\tau, f)$ in (3) is computed for a discrete grid of code delays and Doppler frequencies. For the code delays, this grid is given by: $\tau = m/f_s,\ m = 0, \ldots, \lfloor L_c T_c f_s \rfloor$ ($\lfloor x \rfloor$ means the greatest integer smaller or equal to x); for the Doppler, the grid resolution is $\Delta f = 2/3 L_c T_c N_c$. The precision in the code delay estimation can be improved by interpolation. This paper has explored to methods: **quadratic** and **piecewise linear** interpolation. Let $\tau^* = m^*/f_s$ and f^* be the code delay and Doppler frequency for which the squared crosscorrelation $X_i(\tau, f)$ is maximum, both interpolation methods utilise the values $\{X_i\left((m^*-1)/f_s, f^*\right), X_i\left(m^*/f_s, f^*\right), X_i\left((m^*+1)/f_s, f^*\right)\}$, and their corresponding code delays. With these values, the quadratic interpolation fits a parabola and the final code delay estimate corresponds to the parabola maximum. The piecewise linear constructs a straight line passing by $\sqrt{X_i\left(m^*/f_s, f^*\right)}$ and the minimum of $\sqrt{X_i\left((m^*-1)/f_s, f^*\right)}$ and $\sqrt{X_i\left((m^*+1)/f_s, f^*\right)}$. Then, it builds another straight line passing by the remaining point with the same slope but opposite sign. The final code delay corresponds to the intersection of both lines. The piecewise linear interpolation relies on the fact that the infinite-bandwidth crosscorrelation is triangular. Figure 4 shows the error in the code delay estimation for two interpolation methods, the piecewise

linear interpolation being the most adequate since the simulations consider infinite bandwidth. First investigations with bandlimited receivers suggest that both methods tend to be similar. Nevertheless, piecewise linear interpolation is less computationally demanding and, for that reason, is the one used in the rest of the paper.

In Figure 4, the error of both methods hold a linear trend due to the practical implementation of the crosscorrelation of (3). This crosscorrelation is computed off-line by an algorithm that performs a sequential search in Doppler, and a parallel search in the code delay. The parallel search is carried implemented by means of the discrete Fourier Transform whose length corresponds to a code epoch. Thus, the code search is based on circular convolutions rather than linear ones, i.e. we assume code-epoch periodicity in the signal and in the code replica. Nevertheless, since we use non-commensurate sampling, the sampled signal and code replica do not hold code-epoch periodicity any more. If a serial code search by linear correlation were carried out, the linear trend in the errors would not appear. In any case, this component of the error is very small (smaller than 3% of the chip period). Figure 5 shows the error in the code delay estimation for a HS-GPS receiver with $N_c = 5$, $N_I = 200$ and $\mathrm{P_{FA}} = 10^{-6}$; its sensitivity for $\mathrm{P_D} = 90\%$ becomes $\mathrm{CN_0} = 20$ dBHz, and the sampling frequency is the previously considered one ($f_s = 5.4558$ MHz). The simulated signal is composed of the GPS L1 C/A SV3 signal with a 3.84 chip delay plus noise. The coarse acquisition estimation corresponds to the delay at which the sampled crosscorrelation is maximum $\tau = m^*/f_s$. For high $\mathrm{CN_0}$s, its error is constant since the coarse acquisition obtains the closest value in the code delay grid to the true delay, i.e. $m^* = 21$ or equivalently 3.94 chips. The error of the piecewise linear estimate decreases as the $\mathrm{CN_0}$ increases, and is clearly superior.

4 CNo ESTIMATION

Let $\tau^* = m^*/f_s$ and f^* be the code delay (previous to interpolation) and Doppler frequency at which the ith satellite signal is acquired, and P the mean power of the received signal $x(t)$ within the dwell time, i.e. $\mathrm{P} = \frac{1}{L_c T_c N_c N_I} \int_0^{L_c T_c N_c N_I} |x(t)|^2 \ dt$. The ith satellite $\mathrm{CN_{0}}_i$ estimate is computed as

$$\widehat{\mathrm{CN_{0}}_i} = 10 \ \log_{10} \left(\frac{X_i(\tau^*, f^*) - L_c T_c N_c \mathrm{P}}{(L_c T_c N_c)^2 \mathrm{P} - X_i(\tau^*, f^*)} \ B_n \right). \tag{7}$$

This estimator is obtained by assuming only one satellite signal in noise of equivalent bandwidth B_n, and substituting P and $X_i(\tau^*, f^*)$ by their corresponding statistical mean values. That approximation is valid for large noncoherent integration. The bandwidth B_n accounts for every filtering that could have been done before acquisition; otherwise, $B_n = f_s$. Due to the previous assumptions, this estimator assumes zero multiaccess interference and should be conveniently modified when the near-far problem arises (see Section 5). Figure 6 shows the estimator performance for a HS-GPS receiver with $N_c = 5$, $N_I = 200$, and $\mathrm{P_{FA}} = 10^{-6}$. As in Figure 5, the simulated signal consists of the SV3 signal, with 3.84 chip delay and zero Doppler, plus white noise ($B_n = f_s$ and $f_s = 5.4558$ MHz). As can be noticed, above the receiver sensitivity ($\mathrm{CN_0} = 20$ dBHz) the performance of the estimator is good, the bias being smaller than 1 dB. This bias is related to the losses due to the sampling of the delay-Doppler search space in acquisition: whereas the SV3 Doppler is in the search grid, the code delay is not. Apart from the small bias, the root-mean squared error (RMSE) becomes very close to the Cramer-Rao bound (CRB).

The proposed estimator has shown a high performance for both code delay and Doppler frequency offsets due to the sampled acquisition search. Typical $\mathrm{CN_0}$ estimators, such as the van Dierendoncks' one [15], are very sensible to these offsets and cannot be applied in One-Shot receivers since they can suffer from a bias of more than 20 dB. In the case of van Dierendoncks' estimator, this is due to the use of postcorrelation coherent sums [15].

5 NEAR-FAR PROBLEM

Given the properties of the propagation in dense urban and indoor environments, the near-far problem, i.e. the nonzero multiuser access interference (MAI), arises in many situations and can give rise to a false signal acquisition [8]. The near-far problem lead to the consideration of multiuser detection techniques [9]. Nevertheless, theses techniques are very computationally demanding, so that a previous stage to identify those signals suffering from the near-far problem is desirable. The computational load of the multiuser technique is then reduced since it acts only in those cases.

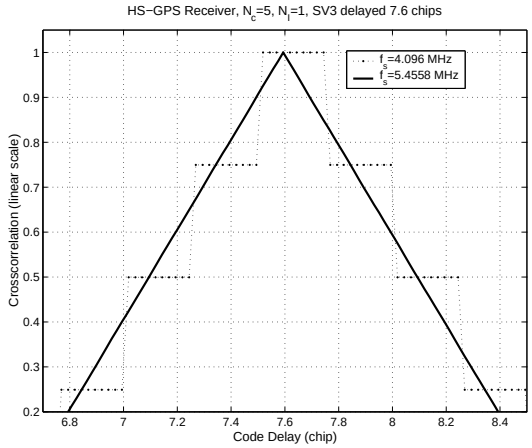

Figure 3: Crosscorrelation for a commensurate and a non-commensurate sampling frequency (noise-free). In abcisas, the delay of the code replica is shown; the input signal holds a code delay of 7.6 chips wrt the time origin.

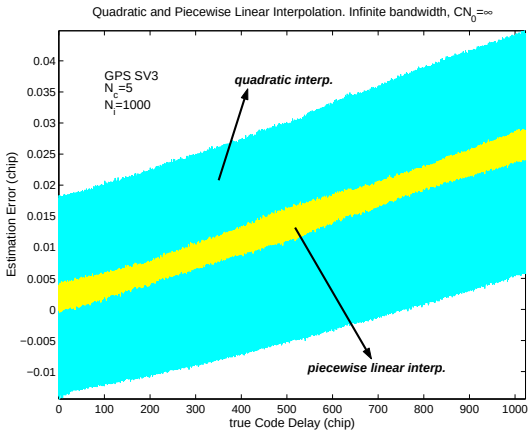

Figure 4: Quadratic and piecewise linear interpolation errors vs. the true code delay of the input signal. HS-GPS receiver, $N_c = 3$, $N_I = 3$; only SV3 present; no noise. Unlimited input bandwidth.

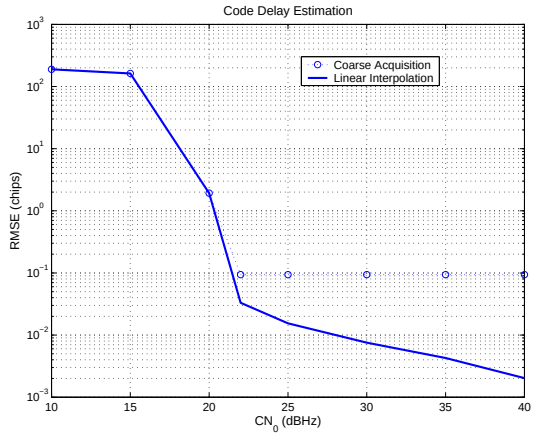

Figure 5: Code Delay Estimation by interpolation vs. the CN_0. HS-GPS receiver, $N_c = 5$, $N_I = 200$, $\mathrm{P_{FA}} = 10^{-6}$; signal composed of SV3 with 3.84 chips code delay, and zero Doppler.

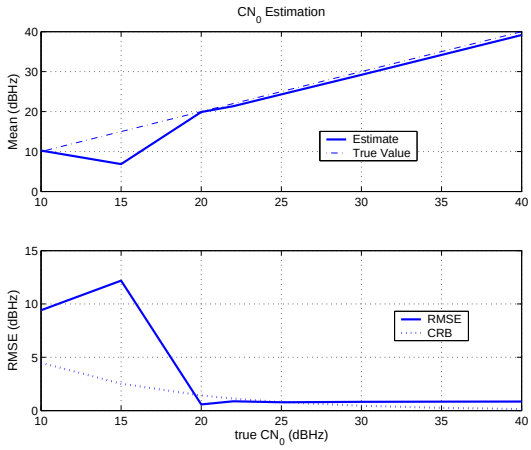

Figure 6: Mean and RMSE of the CN_0 estimator vs. the true CN_0. HS-GPS receiver, $N_c = 5$, $N_I = 200$, $\mathrm{P_{FA}} = 10^{-6}$; signal composed of SV3 with 3.84 chips code delay, and zero Doppler.

The near-far detector is based on the different statistical model of the squared crosscorrelation of (4) for zero and nonzero MAI situations. Let τ^* and f^* be the code delay and Doppler frequency at which the ith satellite signal has been acquired. For zero MAI, the squared correlation $X_i(\tau, f^*)$ will be dominated by the noise for any τ more than one chip away from τ^*. Hence, it will follow a χ^2 distribution of $2N_I$ degrees of freedom (mean $2N_0L_cT_cN_c$, and variance $2N_0L_cT_cN_c/N_I$), and the probability of $X_i(\tau, f*)$ surpassing a given threshold X_{TH} can be theoretically computed. However, for nonzero MAI, $X_i(\tau, f*)$ will be dominated by the crosscorrelation between the interfering signal and the code replica of the ith satellite signal, and its distribution will differ much from the previous theoretical one. Indeed, the probability of $X_i(\tau, f*)$ surpassing a given threshold X_{TH} for nonzero MAI will be much higher than the same probability for zero MAI due to the crosscorrelation properties of the GPS C/A codes. The near-far problem detector is defined as the ratio between the probability of $X_i(\tau, f*)$ surpassing a threshold X_{TH} (for a τ more than one chip away from τ^*) estimated from the computed squared crosscorrelation, and the same probability computed according to the theoretical model for zero MAI. This ratio will be close to unity for zero MAI, and large for nonzero MAI. The near-far problem detector compares the obtained ratio with a threshold P_{TH} to distinguish both situations. A nonzero MAI situation is illustrated in Fig. 7 for a HS-GPS receivers and a signal composed of a strong satellite signal and a weak one. Note, that the estimated probability of surpassing X_{TH} is 4% and the theoretical one is smaller than 10^{-10}. The X_{TH} is selected as 0.5 dB lower than the maximum of the squared correlation ($X_i(\tau^*, f^*)$) and is shown in the figure as well. The mean of $X_i(\tau, f^*)$ has to be estimated as well, since the noise spectral density (N_0) is unknown.

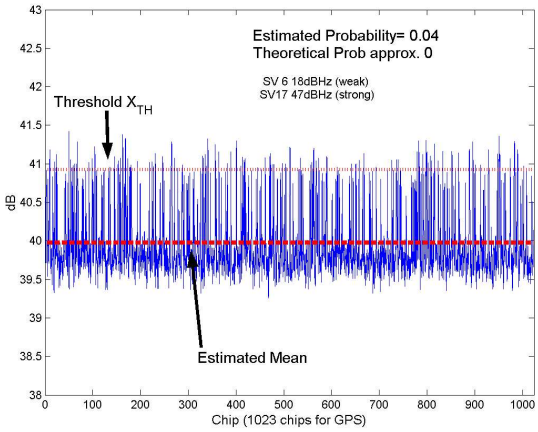

Figure 7: Squared crosscorrelation in the acquisition of SV6; a weak and a strong satellite signals are received. HS-GPS receiver with $N_c = 5$, $N_I = 1000$ and $\mathrm{P_{FA}} = 10^{-6}$; sensitivity $\mathrm{CN_0} = 16$ dBHz ($\mathrm{P_D} = 90\%$).

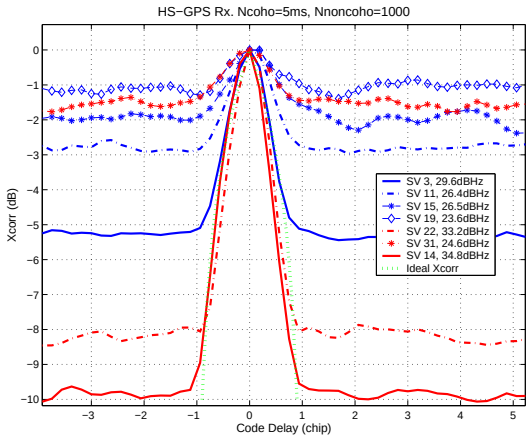

Figure 8: Normalized correlation of the acquired satellites of the indoor dataset A.

The threshold P_{TH} is set to 10.

If the near-far detector finds that a satellite signal is affected by nonzero MAI, the receiver skips the acquisition of that satellite and continues acquiring other visible satellites. When the acquisition has finished, the multiuser technique is applied to each of the skipped satellite signals. The multiuser technique [9, 10] consists of computing the orthogonal complement of the received signal to the subspace spanned by the satellite signals previously acquired holding a high $\mathrm{CN_0}$ estimated value (20 dB over the receiver sensitivity). That is, let $\mathcal{I}$ be the set of satellites fulfilling the former condition, the receiver estimates the code delay and Doppler frequency for each one. The subspace spanned by them is defined as span $\left(\{c_i(t-\widehat{\tau}_i)\ e^{j(2\pi\widehat{f}_i\ t)}\}_{i\in\mathcal{I}}\right)$. Note that, those strong satellite signals cannot be subtracted from the received signal in a straightforward way since the phase offsets $\{\phi_i\}_{i\in\mathcal{I}}$ (see Eqn. 1) cannot be estimated from the squared crosscorrelation of (4).

The orthogonal complement of the received signal is utilised in the acquisition of the satellite signals that were found to be affected by MAI. This acquisition is similar to the one described in Section 3. Nevertheless, the estimation of the $\mathrm{CN_0}$ for these satellite signals uses the mean power (P) of the orthogonal complement instead of the total mean power of the received signal.

6 EXPERIMENTAL RESULTS

Live intermediate frequency GPS samples have been collected by the SampleStreamer of the NordNav R30 software receiver [16], at 16 MHz sampling rate (approximately), 4 MHz intermediate frequency, 3 MHz bandwidth and 4 bits. Off-line preprocessing demodulates, filters, and decimates (by 3: $f_s = 5.4558$ MHz) the sampled signal. The preprocessed environments have been analysed by a One-Shot receiver with the following parameters: $N_c = 5$, $N_I = 1000$, $\mathrm{P_{FA}} = 10^{-6}$, sensitivity $\mathrm{CN_0} = 16$ dBHz (for $\mathrm{P_D} = 90\%$), and piecewise linear interpolation. Both the preprocessing and the receiver have been implemented in Matlab. The results for two indoor datasets are shown in Table 1, and are in accordance with those obtained by the NordNav receiver processing the equivalent outdoor environment. Following the A-GNSS philosophy, the Nordnav receiver itself has been used as a reference receiver, i.e.: Only those satellites detected by the NordNav receiver in the equivalent outdoor environment have been searched for indoors, and the indoor Doppler search is constrained around the frequency estimated by the NordNav receiver outdoors. The degradation in $\mathrm{CN_0}$ for both indoor environments is around 20 dB, and some of the satellites acquired outdoors cannot be detected indoors. The crosscorrelation of the acquired satellites is shown in Fig. 8 for dataset A. After computing the position indoors by means of an A-GNSS location processor as suggested in [12, Category 3], the positioning error is slightly higher than 150 m for both datasets, probably due to the effect of the multipath.

Table 1: Analysis of live GPS indoor environments.

Visible SV (Nordnav)	Code Delay (chips)	Doppler (Hz)	Indoor CN_0 (dBHz)	Outdoor CN_0 (dBHz)
INDOOR DATASET A, 11 June 2004, 8:06am				
3	102.76	-2858.49	29.6	50.6
11	150.63	2265.33	26.4	45.7
14	123.88	2349.37	34.8	45.0
15	583.23	-3379.89	26.5	49.7
19	101.11	-181.48	23.6	50.0
22	356.11	-2242.82	33.2	51.8
31	219.53	2235.88	24.6	48.7
18,28	Not Detected			43.4,44.4
INDOOR DATASET B, 15 June 2004, 10:44am				
1	208.97	3027.33	29.1	45.9
11	955.83	-1876.67	24.2	51.3
19	337.09	-4390.33	35.7	45.2
20	110.76	900.33	34.2	50.9
28	187.37	-3100.00	21.0	43.2
7,14	Not Detected			46.8,48.3

7 CONCLUSIONS: EXTENSION TO GALILEO

A One-Shot receiver for indoor positioning has been studied, and tested with simulated and live GPS indoor samples. It is based on the HS-GNSS principle, and includes piecewise linear interpolation, a novel CN_0 estimator adequate for weak signals, and a near-far problem mitigation technique. The receiver operation is based on A-GNSS and includes an A-GNSS positioning processor. The slightly high positioning errors found in live indoors environments suggest the influence of multipath. A future activity will be the development of a suitable multipath mitigation algorithm.

The operation principles of the proposed receiver are of general nature and, therefore, they are applicable in the same way to Galileo. Galileo will bring a large number of benefits to satellite-based indoor positioning. First of all, the number of available measurements will at least be doubled on average. At present, in deep indoor environments the number of available satellite signals may be less than four, what makes impossible the computation of the position in those circumstances. This will be improved if Galileo and GPS are used simultaneously. In the second place, the Galileo signals contain several features improving the performance of A-GNSS/HS-GNSS receivers. The increase in transmitted power is the most evident advantage. Next, the existence of pilot signals (i.e. signals without data modulation) will make possible to extend the coherent correlation time without data aided techniques, and the losses caused by bit transitions will be avoided. Finally, Galileo signals will have longer codes, which is doubly advantageous: 1) The cross-correlation between signals diminishes (more robustness to the near-far problem), and 2) the ambiguity in the pseudorange measurements performed by the A-GNSS positioning processor is also reduced and the computation of the GNSS time will be easier [12]: This will lead either to relaxed synchronisation requirements between the receiver time and the GNSS time for A-GNSS systems, e.g. in 3G mobile networks, in that the receiver is maintained tightly synchronised to GNSS time, or to a reduced complexity in the computation of the position for A-GNSS systems, e.g. in GSM mobile networks, in that the synchronisation to the A-GNSS is not very tight and the receiver itselt has to solve for the ambiguity in the pseudoranges by computing the least-square residuals within the clock uncertainty range (see [12, Category 3]).

REFERENCES

[1] F. van Diggelen and C. Abraham. Indoor GPS: The Non-Chip Challenge. *GPS World*, Sept. 2001.

[2] J. LaMance, J. DeSalas, and J. Jarvinen. Assited-GPS: A Low-Infrastructure Approach. *GPS World*, March 2002.

[3] K. Pahlavan, X. Li, and J.-P. Mäkelä. Indoor Geolocation Science and Technology. *IEEE Communications Magazine*, pages 112–118, Feb 2002.

[4] Coordination Group on Access to Location Information for Emergency Services (CGALIES). Work Package 1. Technical report, CGALIES, 2002. *http://www.telematica.de/cgalies*.

[5] F. van Diggelen. Indoor GPS Theory & Implementation. In *Proc. IEEE Position, Location & Navigation Symposium 2002*, pages 240–247, 2002.

[6] Coordination Group on Access to Location Information for Emergency Services (CGALIES). Implementation Issues related to Access to Location Information by Emergency Services (e112) in the European Union. Technical report, CGALIES, 2002. *http://www.telematica.de/cgalies/main.html*.

[7] G. Lachapelle, H. Kuusniemi, D. T. H. Dao, G. MacGougam, and M. E. Cannon. HSGPS Signal Analysis and Performance under Various Indoor Conditions. *Navigation: Journal of The Institute of Navigation*, 51(1):29–43, 2004.

[8] G. P. Mattos. Solutions to the Cross-Correlation and Oscillator Stability Problems for Indoor C/A Code GPS. In *Proc. ION GPS/GNSS 2003*, pages 654–659, Sept 2003.

[9] S. Verdu. *Multiuser Detection*. Cambridge University Press, 1998.

[10] P. H. Madhani, P. Axelrad, K. Krumvieda, and J. Thomas. Application of Successive Interference Cancellation to GPS Pseudolite Near-Far Problem. *IEEE Trans. on Aerospace and Electronic Systems*, 39(2):481–488, April 2003.

[11] N. Agarwal et al. Algorithms for GPS Operation Indoors and Downtown. *GPS Solutions*, 6(3):149–160, December 2002.

[12] J. Syrjärinne. Possibilities for GPS Time Recovery with GSM Network Assistance. In *Proc. ION GPS*, pages 955–966, Sept 2000.

[13] L. Vittorini and B. Robinson. Frequency Standards: Key Enablers to Optimizing Indoor GPS Performance. In *Proc. ION GPS/GNSS 2003*, pages 660–678, Sept 2003.

[14] K. J. Quirk and M. Srinivasam. Analysis of Sampling and Quantization Effects on the Performance PN Code Tracking Loops. In *Proc. IEEE Int. Conference on Communications*, volume 3, pages 1480–1484, April-May 2002.

[15] B. W. Parkinson and J. J. Spilker, editors. *Global Positioning System: Theory and Applications*, volume 1. American Institute of Aeronautics and Astronautics, 1996.

[16] NordNav Technologies. Product catalog: Nordnav R30^{TM}. *http://www.nordnav.com*, 2004.